Development of a simulation tool coupling hydrodynamics and unsteady aerodynamics to study Floating Wind Turbines

Leroy Vincent, Jean-Christophe Gilloteaux, Maxime Philippe, Aurélien Babarit, Pierre Ferrant

DEVELOPMENT OF A SIMULATION TOOL COUPLING HYDRODYNAMICS AND UNSTEADY AERODYNAMICS TO STUDY FLOATING WIND TURBINES

Vincent LEROY
LHEEA Lab., Ecole Centrale Nantes – CNRS
INNOSEA
1 rue de la Noë, 44000 Nantes, France
vincent.leroy@ec-nantes.fr

Jean-Christophe GILLOTEAUX
LHEEA Lab., Ecole Centrale Nantes – CNRS
1 rue de la Noë, 44000 Nantes, France
jean-christophe.gilloteaux@ec-nantes.fr

Maxime PHILIPPE
INNOSEA
1 rue de la Noë, 44321 Nantes, France

Aurélien BABARIT
LHEEA Lab., Ecole Centrale Nantes – CNRS
1 rue de la Noë, 44000 Nantes, France

Pierre FERRANT
LHEEA Lab., Ecole Centrale Nantes – CNRS
1 rue de la Noë, 44000 Nantes, France

ABSTRACT

Depending on the environmental conditions, floating Horizontal Axis Wind Turbines (FHAWTs) may have a very unsteady behaviour. The wind inflow is unsteady and fluctuating in space and time. The floating platform has six Degrees of Freedom (DoFs) of movement. The aerodynamics of the rotor is subjected to many unsteady phenomena: dynamic inflow, stall, tower shadow and rotor/wake interactions. State-of-the-art aerodynamic models used for the design of wind turbines may not be accurate enough to model such systems at sea. For HAWTs, methods such as Blade Element Momentum (BEM) [1] have been widely used and validated for bottom fixed turbines. However, the motions of a floating system induce unsteady phenomena and interactions with its wake that are not accounted for in BEM codes [2]. Several research projects such as the OC3 [3], OC4 [4] and OC5 [5] projects focus on the simulation of FHAWTs.

To study the seakeeping of Floating Offshore Wind Turbines (FOWTs), it has been chosen to couple an unsteady free vortex wake aerodynamic solver (*CACTUS*) to a seakeeping code (*InWave* [6]). The free vortex wake theory assumes a potential flow but inherently models rotor/wake interactions and skewed rotor configurations. It shows a good compromise between accuracy and computational time.

A first code-to-code validation has been done with results from *FAST* [7]on the FHAWT OC3 test case [3] considering the NREL 5MW wind turbine on the OC3Hywind SPAR platform. The code-to-code validation includes hydrodynamics, moorings and control (in torque and blade pitch). It shows good agreement between the two codes for small amplitude motions, discrepancies arise for rougher sea conditions due to differences in the used aerodynamic models.

NOMENCLATURE

M	Mass matrix of the system ($kg, kg.m^2$)
M_{a_∞}	Added mass at infinite frequency ($kg, kg.m^2$)
$x(t)$	Position of the system at time t (m, rad)
K_{rad}	Radiation impulse response ($N/m.s^{-1}, N/rad.s^{-1}$),
K_h	Hydrostatic stiffness matrix ($N.m^{-1}, N.m/rad$)
F_{FK}	Froude-Krylov force ($N, N.m$)
K_{diff}	Diffraction loads impulse response
$\eta(t)$	Free surface elevation at reference point (m)
$F_{moor.}$	Mooring loads ($N, N.m$)
F_{aero}	Aerodynamic loads ($N, N.m$)
Γ_B	Bound vorticity (s^{-1})
c	Element chord (m)
U_e	Wind velocity on blade element ($m.s^{-1}$)
U_∞	Free stream wind velocity at hub height ($m.s^{-1}$)
C_L	Lift coefficient
C_D	Drag coefficient

C_M	Moment coefficient
C_P	Power coefficient
C_T	Thrust coefficient
T, T_p	Regular wave period, wave peak period (spectrum) (s)
H, H_s	Regular wave height, significant height (spec.) (m)
γ	Peakness factor used in JONSWAP spectrum

INTRODUCTION

A lot of research has focused over the last decade on Floating Offshore Wind Turbines (FOWTs). State-of-the-art models used to model the aerodynamics of such turbines assume a potential steady flow on the rotor. The Blade Element Momentum (BEM) method is hence mainly used [1] for Horizontal Axis Wind Turbines (HAWTs). However, such floating systems have a very unsteady behaviour at sea. The six Degrees of Freedom (DoFs) of the platform induce a complex flow around the rotor, the inflow is unsteady and stall can occur on the blades. Also, if the platform's pitch motion is important, skewed rotor configurations can occur and the BEM method is not accurate in this configuration. Recent research showed that unsteady phenomena that are not modelled in the BEM method are important to consider for FOWTs when they are moving in surge and pitch [2] [8] and when skewed rotor configurations occur [9].

The use of a free vortex method has been chosen to model the unsteady aerodynamics of FOWTs for the present development. This method shows a good compromise between computational cost and unsteady aerodynamic loads accuracy. *CACTUS* [10] is a lifting-line free vortex wake method that has been implemented at the Sandia National Laboratories (SNL) (USA). It has been coupled in a modular framework to *InWave* [6], a seakeeping code developed at INNOSEA (Nantes, France) in collaboration with the LHEEA Lab of the Ecole Centrale de Nantes. *InWave* integrates the linear potential flow solver *Nemoh*, developed at the Ecole Centrale de Nantes and solves the equation of motion in time domain through a multi-body algorithm. It also accounts for regular and irregular waves and quasi-static mooring.

This paper presents the coupled method and the work of verification lead on the OC3 test case [3], considering the NREL 5MW HAWT designed at the National Renewable Energy Laboratory (NREL) on the OC3Hywind SPAR. The results from *InWave-CACTUS* were compared with those from FAST [7]. The coupled method showed good agreement with the results from FAST for small amplitude motions. Discrepancies appear in skewed rotor configurations and when the rotor/wake interactions are strong.

DESCRIPTION OF THE NUMERICAL MODEL

Hydrodynamics and multi-body solver

The equation of motion is solved by *InWave* [6], developed at INNOSEA in collaboration with the LHEEA Laboratory at the ECN. *InWave* includes a time-domain multi-body solver, coupled to the linear potential flow solver *Nemoh* [11] developed at the ECN. *Nemoh* computes the first-order hydrodynamic loads (excitation force, diffraction, radiation damping and added-mass). The equation of motion of a floating system can be written as follows [12]:

$$
\begin{aligned}
\left(M + M_{a_\infty}\right)\ddot{x}(t) &+ \int_0^t K_{rad}(\tau)\dot{x}(t-\tau)d\tau + K_h x(t) \\
&= F_{FK} + \int_{-\infty}^{+\infty} K_{diff}(\tau)\eta(t-\tau)d\tau + F_{moor.} \\
&+ F_{aero.}
\end{aligned}
$$

InWave was initially developed to model Wave Energy Converters (WEC). The multi-body algorithm comes from robotics, considers relative degrees of freedom (DOF) and coordinates and thus decreases the number of equations to be solved [13]. This is adapted for floating wind turbines as we consider a rotating body (the rotor) on a free floating platform. *InWave* also computes quasi-static mooring loads through *MAP++* [14]. *InWave* has been validated through a code-to-code and experimental validation [15] [16]. All bodies are rigid in the present study.

Unsteady aerodynamics solver

State-of-the-art models used to design FOWTs are based on Froude-Rankine actuator disk theory. The Blade Element theory assumes that each blade element is submitted to a 2D flow. BEM theory couples these two assumptions. Semi-empirical models can be added to account for unsteady phenomena such as tip and hub losses, dynamic inflow and dynamic stall. However, the assumption of steady flow is hardly valid for such floating turbines as the sources of unsteady phenomena are numerous: the inflow is unsteady because of atmospheric turbulence and wind-wave interactions; the blades experience tip vortices and dynamic stall due to pitch rate effects and pitch control. The rotor strongly interacts with its wake and the tower sheds vortices in the wake. The overall motion contributes as well in inducing unsteadiness.

It has been chosen in this study to use a lifting-line free vortex wake method. This theory assumes potential flow but is inherently unsteady, making computational times longer than steady models. Blade Element theory is used with the aerodynamic lift, drag and moment coefficients C_L, C_D and C_M. The method is thus limited to known profiles. Each element generates a bound vortex according to Kutta-Joukowski equation. A bound vorticity Γ_B is calculated from the element chord c, the wind velocity on blade element U_e and the lift coefficient C_L.

$$
\Gamma_B = \frac{1}{2}cU_e C_L
$$

Helmholtz theorem (conservation of vorticity along a vortex line) links this bound vorticity to trailing and span-wise vortices in a lattice as shown in Figure 1 (from [10]). These vortex lines induce a velocity in the blade element inflow U_e by application of the Biot-Savart law. Iterations are thus needed between Kutta-Joukowski and Biot-Savart laws until the bound

vorticity converges. Eventually, at the end of each time step, the vortex lines are advected at local wind speed (i.e. accounting for vorticity). Tip vortex losses and skewed rotor configurations are inherently accounted for in lifting-line free vortex wake theory; it thus shows better results than BEM codes in yawed rotor configurations [9].
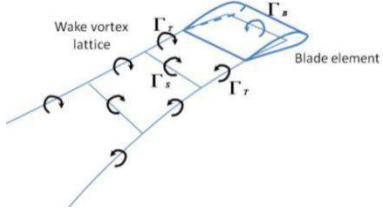

Figure 1: Vortex lattice in free vortex Wake Method from [10]

Additionally, viscous phenomena such as dynamic inflow can be accounted for using semi-empirical models such as Boeing-Vertol or Leishman Beddoes, as presented in [10].

CACTUS [10] is such an open-sources code and has been developed at Sandia National Laboratories (USA). It has been validated on either fixed horizontal or vertical axis rotors as presented in [10].

Servo-Hydro-Aerodynamics coupling

InWave and *CACTUS* have been coupled in a modular framework. At each time step *CACTUS* computes the aerodynamic loads on each blade element and *InWave* solves the motion equation accounting for hydrodynamics, mooring and generator control. Blade pitch control is also considered through an external module. Blades are considered rigid for now. A scheme of the modular framework is presented in Figure 2.
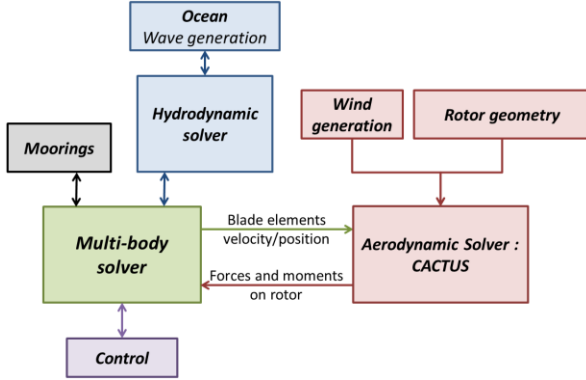

Figure 2: Modular framework coupling *InWave* and *CACTUS*

At each time-step, *InWave* sends to *CACTUS* the position and velocities of all elements (including velocity induced by the structure's motion), and the orientation of the blade elements accounting for control. *CACTUS* computes the aerodynamic loads and sends back the forces and moments acting on the rotor, used to solve the motion equation in *InWave*.

The control module is independent, and can account for any quantity coming from the multi-body time domain solver. It can thus focus on rated speed/torque, but also on tensions in mooring lines, motion amplitude, hub speed, or other.

VALIDATION ON THE OC3 TEST CASE

A first verification has been done on the fixed NREL 5MW rotor presented in [17] at several Tip-Speed Ratios (TSRs), with constant rotational speed and without blade pitch control. The aerodynamic thrust and power coefficients from *InWave-CACTUS* were compared with those from *FAST*. *AeroDyn* [1] is *FAST*'s aerodynamic solver. It is based on BEM method, assuming steady flow. The used version of *AeroDyn* does not account for Generalized Dynamic Wake (GDW) model. Tip losses are modelled in *FAST* using the Prandtl model. The comparison showed good agreement but it is not presented here. The same 2D aerodynamic coefficients and blade discretization presented in [17] were used in the two codes and convergence was verified in terms of rotor thrust and power coefficients. Dynamic stall was disabled.

The Offshore Code Comparison Collaboration (OC3) gathered developers of design tools for floating wind turbines and worked on several test cases. In the following, we focus on the Phase IV concerning the floating SPAR OC3Hywind supporting the NREL 5MW HAWT, as described in [3].

The SPAR buoy is 120m draft, moored with 3 catenary lines, and Morison drag is considered on the platform with a $C_D = 0.6$ drag coefficient. The rotor is 63m radius; its hub is at $90\ m$ height with a 5° shaft tilt. The effect of the tower on the aerodynamics is not modelled. The main parameters of the floating system are defined in [3] and presented in Table 1. The OC3 project includes several load cases that were treated in this study. They are described in Table 2.

Table 1: Main parameters of the floating system

Depth	$320\ m$
Draft	$120\ m$
Platform, tower and nacelle mass	$7956\ t$
Rotor mass	$110\ t$
Surge resonance period	$125\ s$
Heave resonance period	$31\ s$
Pitch resonance period	$30\ s$
Rotor radius	$63m$
Hub height	$90\ m$
Shaft tilt	5°
Rated wind speed	$11.4\ m.s^{-1}$
Rated rotational speed	$12\ RPM$
Fairlead depth	$-70\ m$
Lines length	$902,2\ m$
Linear mass	$77,066\ kg/m$
Axial stiffness	$384,243\ MN$
Line diameter	$0,09\ m$

The validation is done comparing the results from *InWave-CACTUS* with those from *FAST*. The time-step used in *InWave* is $0.2\ s$. It is ensured that the motions and the aerodynamic loads are converged. The hydrodynamic impulse responses have a time-step of $0.0125\ s$. *FAST*'s time step is $0.0125\ s$ to ensure a sufficiently small time-step for impulse responses.

Table 2: Load cases used in the code-to-code validation

Load Case	Analysis	Wind Conditions	Wave conditions
1	Equilibrium position	Air density = 0	Still water
2	Decay	Air density = 0	Still water
3	Time-series	Air density = 0	Airy wave: $H = 6\,m, T = 10\,s$
4	PSD	Air density = 0	JONSWAP wave spectrum: $H_s = 6\,m, T_P = 10\,s$
5	Time-series	Steady, uniform, no shear: $U_\infty = 8\,m.s^{-1}$	Airy wave: $H = 6\,m, T = 10\,s$
6	Time-series	Steady, uniform, no shear: $U_\infty = 18\,m.s^{-1}$	Airy wave: $H = 6\,m, T = 10\,s$
7	PSD	Turbulent, Kaimal spectrum: $U_\infty = 11.4\,m.s^{-1}$	JONSWAP wave spectrum: $H_s = 6\,m, T_P = 10\,s$
8	PSD	Turbulent, Kaimal spectrum: $U_\infty = 18\,m.s^{-1}$	JONSWAP wave spectrum: $H_s = 6\,m, T_P = 10\,s$

In calm conditions, *CACTUS* and *AeroDyn* may have similar results, but differences are expected to grow when unsteady phenomena occur, when the motion amplitudes are large for instance because the steady assumption may not be valid anymore. It is also pointed out that the BEM method is not stable at high TSRs. The hydrodynamic module of *FAST* is *HydroDyn* [18]. It computes first-order hydrodynamic loads and Morison drag is computed at the equilibrium position. That means that relative fluid velocity is computed at the static equilibrium position of each element while *InWave* uses the instantaneous position of the Morison elements that are under water only. This may cause a viscous drift on the SPAR platform [19]. The same control DLL provided with FAST is used for generator torque and blade pitch.

In the first place, once the equilibrium position is computed, the hydrodynamic and mechanical model is verified without wind through decay tests and simulations in regular and irregular waves. Eventually, servo-hydro-aerodynamic simulations are run with regular and irregular waves, constant wind and turbulent wind computed with a Kaimal spectrum. All bodies are assumed to be rigid. Hydrostatic loads in *InWave* can either be linear (using hydrostatic stiffness matrix K_h) or non-linear, i.e. the hydrostatic pressure field is integrated on the instantaneous wetted surface of the platform. It is chosen to use non-linear hydrostatics in the following.

Decay tests

Three decay tests are simulated with 6 DOF, respectively for an initial platform surge of $x_0 = 20$m, heave of $z_0 = 5$m and pitch of $\theta_0 = 10°$. Surge, heave and pitch time-series are respectively plotted from Figure 3 to Figure 5: surge, heave and pitch obtained from the respective decay tests. A very good agreement is observed.
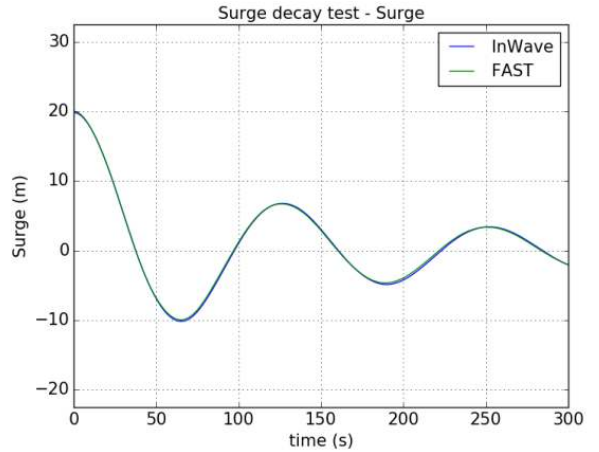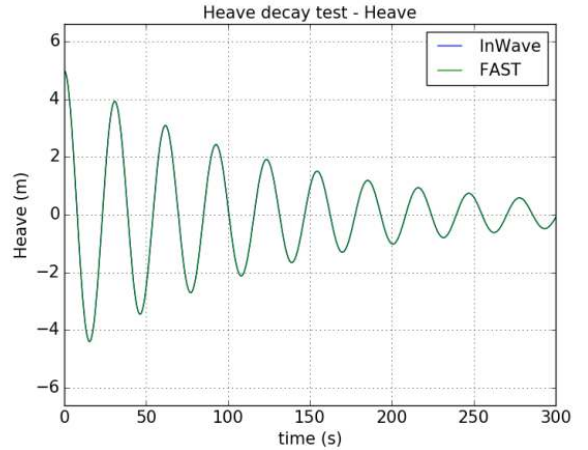

Figure 3: Surge decay test
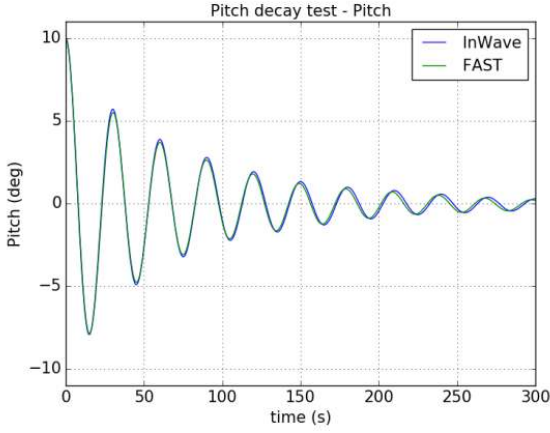

Figure 4: Heave decay test
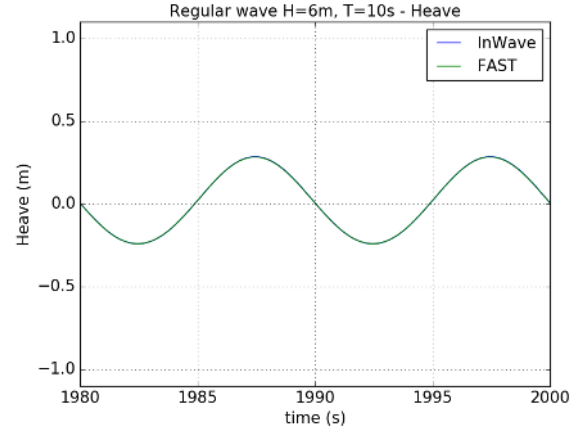
4

Figure 5: Pitch decay test

Figure 7: Regular waves – Heave

Regular waves

Regular waves are now generated to see how the floating and moored structure responds. The wave period is $T = 10s$ and the wave height is $H = 6m$ and it propagates in the x direction. Surge, heave and pitch time-series are plotted from Figure 6 to Figure 8. Very good agreement is obtained between *FAST* and *InWave*.

Irregular waves

Irregular waves are now generated with a JONSWAP spectrum considering $T_p = 10s$, $H_s = 6m$ and $\gamma = 3.3$. The free surface elevation computed with *InWave* is imported within *HydroDyn*. Morison drag is disabled here in order to have the same hydrodynamic models and to avoid viscous drift. Power Spectral Density (PSD) on 4000s time series is computed (out of a total of 8000s to avoid transient effects). Results from *InWave* and *FAST* are plotted and compared from Figure 9 to Figure 11. Results show very good agreement.

Figure 8: regular waves – Pitch

Figure 6: Regular waves - Surge
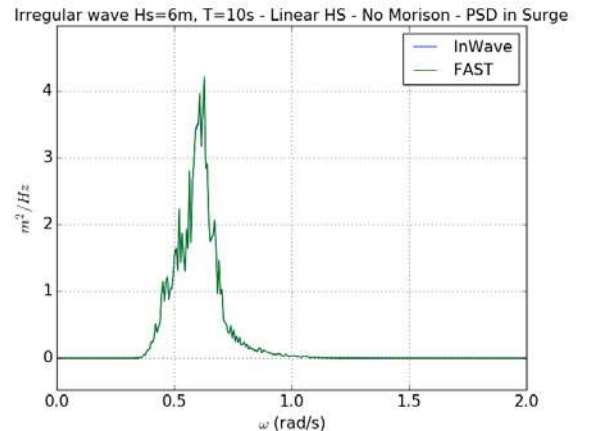
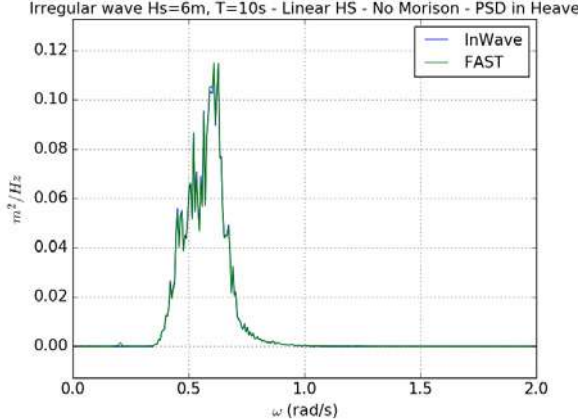**Figure 9: Irregular waves - PSD in Surge**

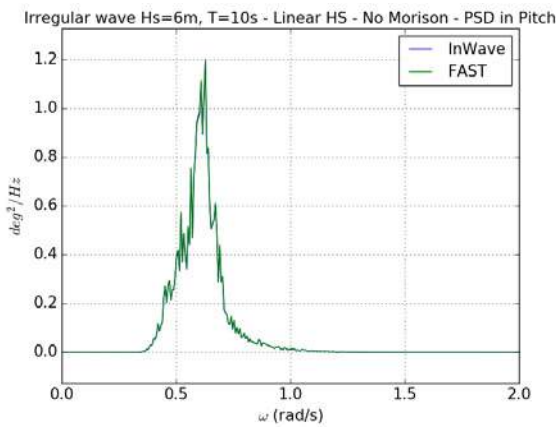**Figure 10: Irregular waves - PSD in Heave**

Figure 11: Irregular waves - PSD in Pitch

Regular waves and constant wind

Wind is now generated. In the first place, constant wind is used without shear effects. The regular wave is the same as previously ($T = 10s$, $H = 6m$) and the wind speed is $U_\infty = 8m.s^{-1}$. The presence of wind shear was ignored. The TSR is high, about 7.5, in this area. Here $C_P = 0.5$ and $C_T = 0.8$.

The motion time series (surge, heave and pitch), rotor speed and aerodynamic thrust are plotted from Figure 12 to Figure 16. The blade pitch control is not active at this wind speed. One can see that the results do not agree perfectly between *InWave* and *FAST*. The amplitudes of motions are similar but the platform has a $1.3\,m$ surge offset and a $0.3°$ pitch offset. The thrust and torque calculated by *CACTUS* are a bit higher (7% relative difference between the mean thrusts), which affect the platform surge, pitch and rotor speed (4% relative difference between the mean rotor speeds). Table 3 sums up the relative differences ϵ obtained between the two models amplitudes and mean values, ϵ being defined as follow for a quantity X:

$$\epsilon = \frac{|X_{InWave} - X_{FAST}|}{|X_{FAST}|}$$

It is known that the BEM method is not stable at high TSRs [1]. At $U_\infty = 8\,m.s^{-1}$ the TSR is about 7.5. The rotor is highly loaded and can experience recirculation flows at its blades tips. Usually, Glauert's empirical formula is used in *AeroDyn* in this case but it may not be accurate enough as explained in [20].

Also, the platform's tilt at $8\,m.s^{-1}$ induces a skewed rotor configuration, in which lifting-line free vortex wake codes are known to be more accurate [9]. Indeed, the rotor plane angle with the vertical plane, including platform pitch (2.7°) and shaft tilt (5°) is about 7.7°. The BEM was used here in *FAST*. The Generalized Dynamic Wake theory could be tested but it may not be more accurate in this case because the GDW was developed for lightly loaded rotors (which is not the case at $U_\infty = 8\,m.s^{-1}$ as presented before). Also, the GDW assumes that induced velocities are small compared to the mean flow, which is not the case at low wind speed when the rotor approaches the turbulent wake state [1]. Additionally, differences between the two models may come from the non-linear hydrostatics used in *InWave* as the platform pitch is higher at $8\,m.s^{-1}$.

Another test was run at a lower TSR, where blade pitch control intervenes, with a $U_\infty = 18\,m.s^{-1}$ constant wind speed. At this TSR, the results show a much better agreement as shown from Figure 17 to Figure 22. Indeed, at low TSR, the interaction between the rotor and its wake is less important. Also, the blade pitch control drives the generator torque and corrects the aerodynamic discrepancies by setting the blades pitch.

Relative difference ϵ between		
	Amplitudes	Mean values
Surge	1.9%	9.1%
Heave	2.0%	15.9%
Pitch	1.2%	9.5%
Rotor speed	15.3%	4.2%
Thrust	7.1%	5.9%

Table 3: Relative difference between the two codes at TSR=7
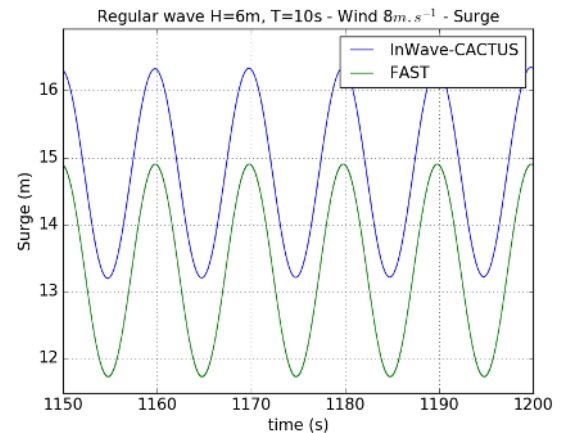

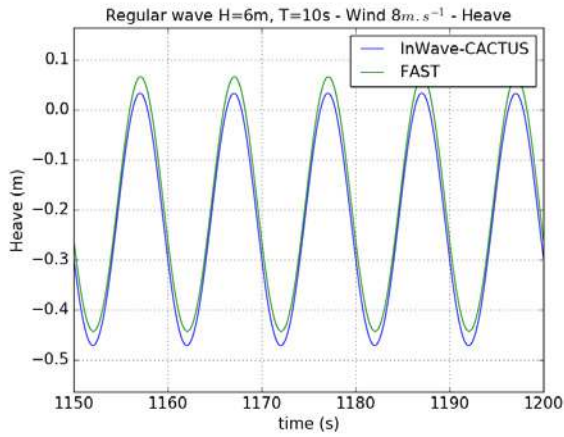**Figure 12: Regular waves and constant $8\,m.s^{-1}$ wind – Surge**

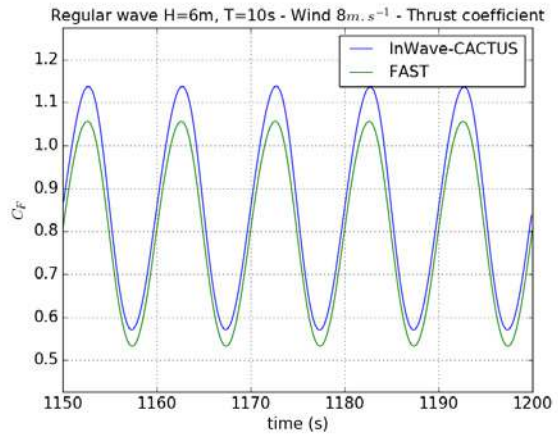**Figure 13: Regular waves and constant 8 $m.s^{-1}$ wind – Heave**

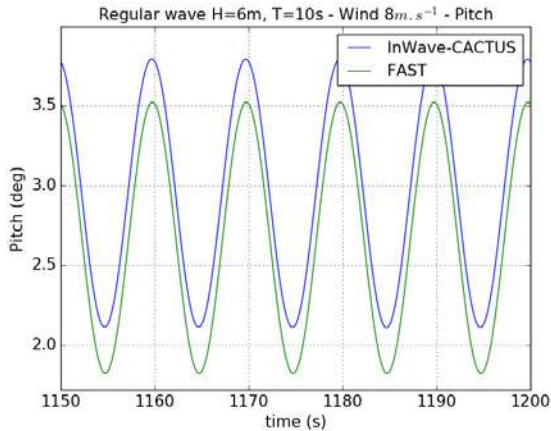**Figure 16: Regular waves and constant 8 $m.s^{-1}$ wind – Thrust coefficient**

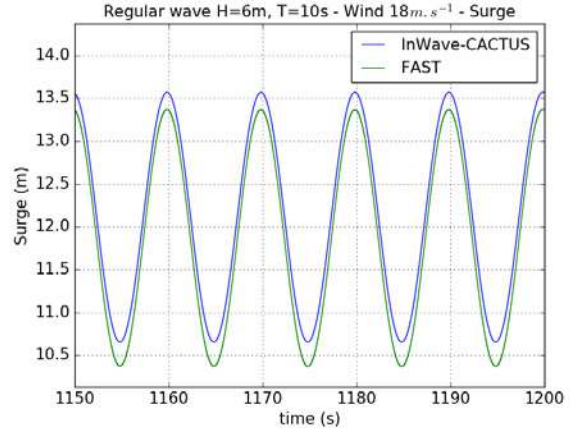**Figure 14: Regular waves and constant 8 $m.s^{-1}$ wind – Pitch**

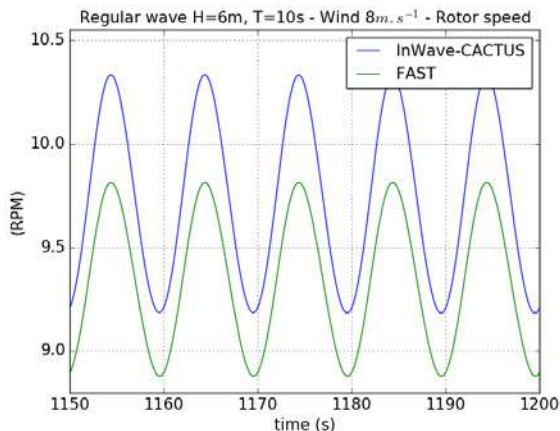**Figure 17: Regular waves and constant 18 $m.s^{-1}$ wind – Surge**

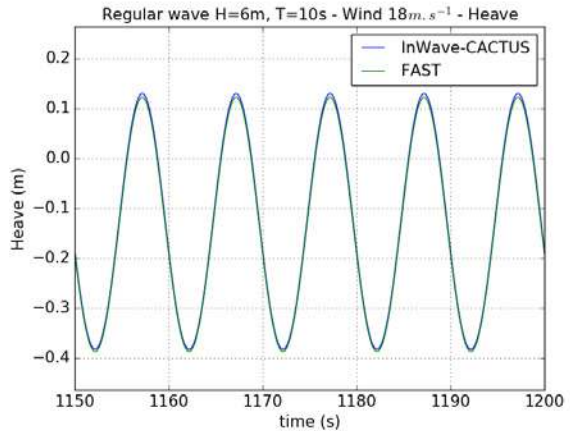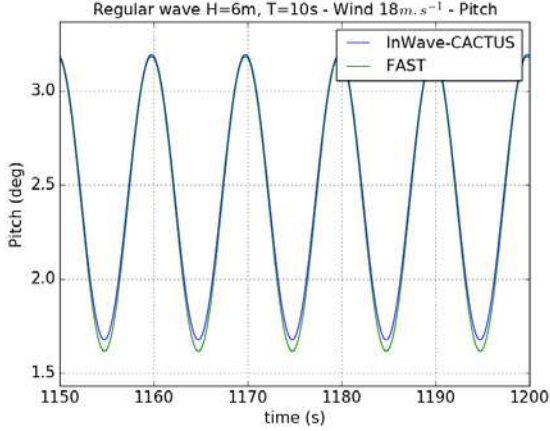**Figure 15: Regular waves and constant 8 $m.s^{-1}$ wind – Rotor speed**

Figure 18: Regular waves and constant 18 $m.s^{-1}$ wind – Heave
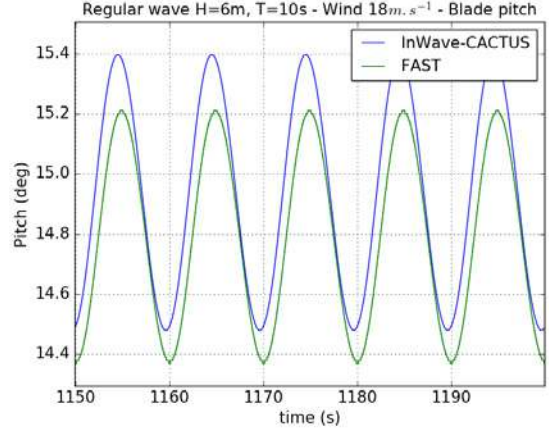
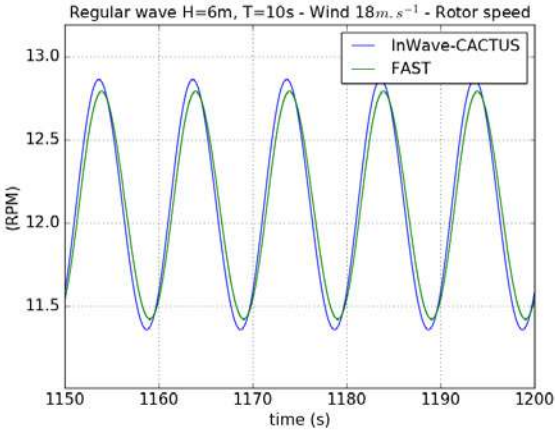**Figure 19: Regular waves and constant $18\ m.s^{-1}$ wind – Pitch**

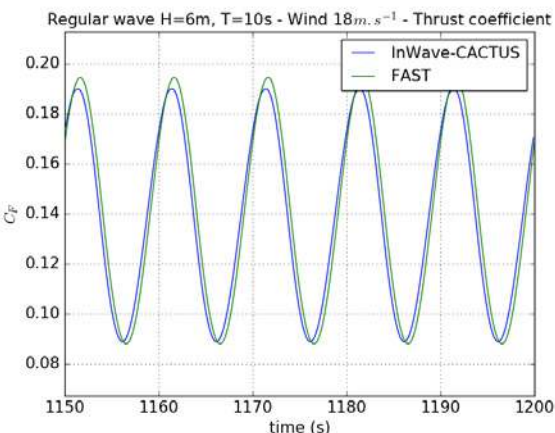**Figure 20: Regular waves and constant $18\ m.s^{-1}$ wind – Rotor speed**

Figure 21: Regular waves and constant $18\ m.s^{-1}$ wind – Thrust coefficient

Figure 22: Regular waves and constant $18\ m.s^{-1}$ wind – Blade pitch

Irregular waves and irregular wind

Irregular waves and irregular wind are generated. Wind turbulence is computed with a Kaimal Spectrum by using *TurbSim* [21]. The irregular wave spectrum is the same as in the previous part: $T_p = 10s$, $H_s = 6m$ and $\gamma = 3.3$.

In the first place, the hub height mean wind speed is $U_\infty = 11.4 m.s^{-1}$. At this rated wind speed, the blade pitch control acts sometimes, as soon as the rated torque is exceeded. The *InWave* free-surface elevation time-series is imported in *FAST*. The motion PSDs are presented from Figure 23 to Figure 25. One can see that a good agreement is obtained between the two codes. The Surge PSD is mostly low-frequency: it is the mooring response. A zoom-in on the wave frequencies would show a good agreement. The pitch PSD shows some discrepancies. They are due to differences in the aerodynamic solvers. These differences are expected at this TSR (about 7) as the rotor strongly interacts with its wake. Also, the sporadic blade pitch control may involve important blade pitch rates that can vary between the two models, and induce important differences in the aerodynamic loads.

Another test has been run with a Kaimal spectrum at a $18\ m.s^{-1}$ mean hub height wind speed. At the $12\ RPM$ rated rotor speed, that gives a 4.4 TSR. At this TSR, $C_P = 0.25$ and $C_T = 0.4$. As previously discussed, the interaction with the wake at this wind speed is much less important. The accordance been *FAST* and *InWave* is then better. The pitch PSD is plotted on Figure 26. Also, a comparison of platform pitch and rotor speed at the two different wind speeds $U_\infty = 11.4\ m.s^{-1}$ and $18\ m.s^{-1}$ is given from Figure 27 to Figure 30. One can see that the agreement in time-series is much better at low TSR.

These results give confidence in the coded coupled environment, as the BEM method is more reliable at lower TSR when rotor-wake interactions are weaker.
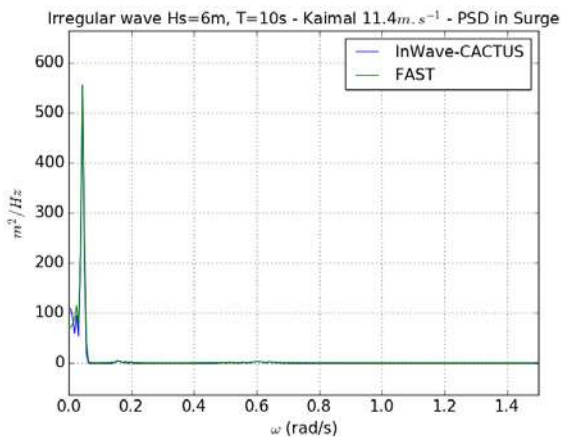
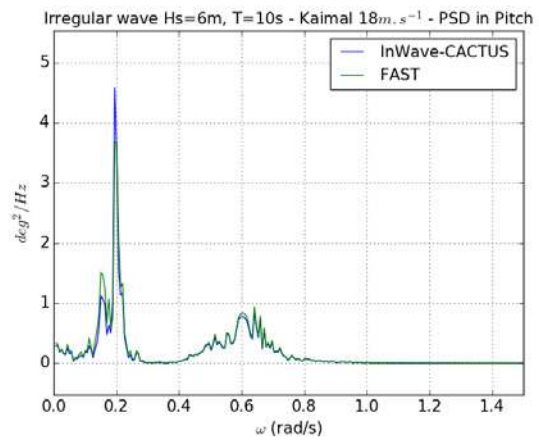**Figure 23: Irregular waves and wind $11.4\ m.s^{-1}$ – Surge PSD**

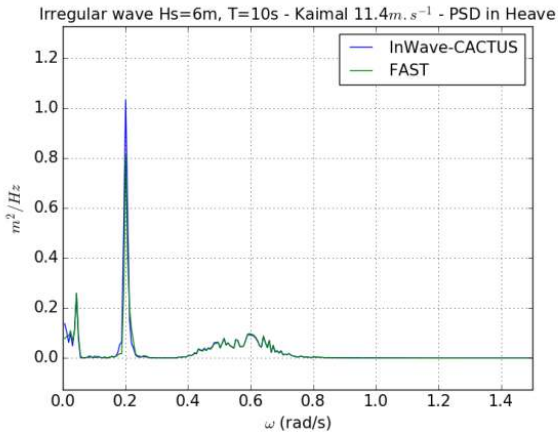**Figure 26: Irregular waves and wind $18\ m.s^{-1}$ – Pitch PSD**

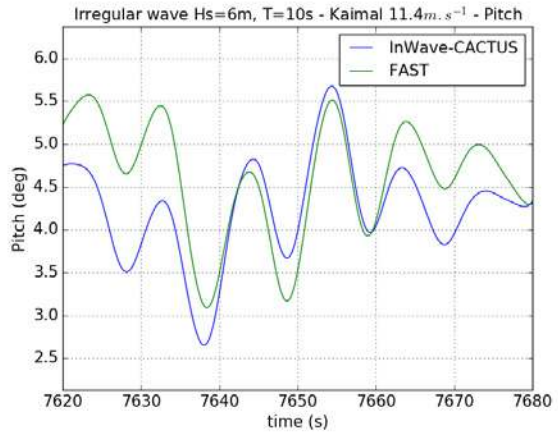**Figure 24: Irregular waves and wind $11.4\ m.s^{-1}$ – Heave PSD**

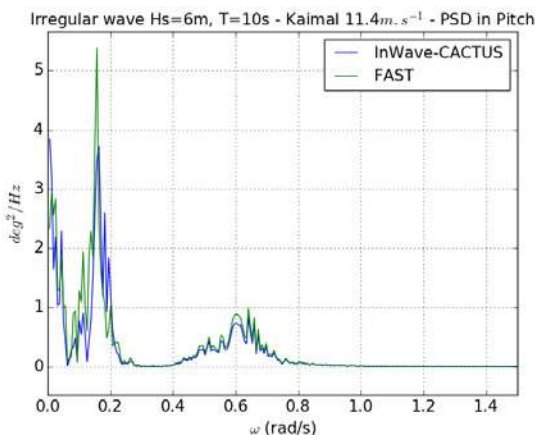**Figure 27: Irregular waves and Kaimal wind $U_\infty = 11.4\ m.s^{-1}$ – Pitch**

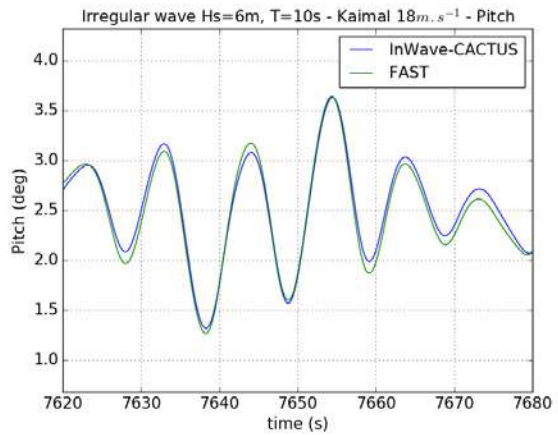**Figure 25: Irregular waves and wind $11.4\ m.s^{-1}$ – Pitch PSD**

Figure 28: Irregular waves and Kaimal wind $U_\infty = 18\ m.s^{-1}$ – Pitch
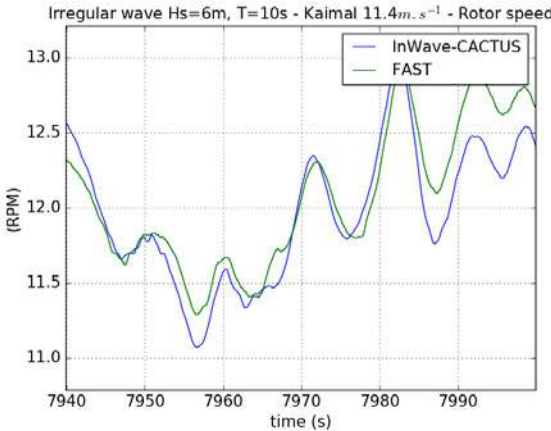
Figure 29: Irregular waves and Kaimal wind $U_\infty = 11.4 \text{ m.s}^{-1}$ – Rotor speed
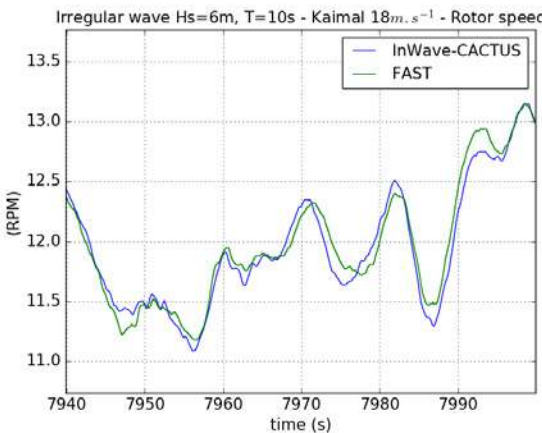

Figure 30: Irregular waves and Kaimal wind $U_\infty = 18 \text{ m.s}^{-1}$ – Rotor speed

CONCLUSION

A new servo-hydro-aerodynamic coupled simulation tool has been presented in this paper. The aerodynamic solver is inherently unsteady which improves the accuracy of calculations of floating wind turbines. The Free Vortex Wake method is flexible and can include semi-empirical models to account for viscous phenomena such as dynamic stall. The wind generation module can consider constant or turbulent inflow, innovative wind models for Offshore Wind Turbines could thus be tested.

A first code-to-code validation with *FAST* has been performed on the OC3 test case considering the OC3Hywind SPAR platform supporting the NREL 5MW HAWT. Several cases were studied, including hydrodynamics-only simulations, servo-hydro-aerodynamic simulations in constant and turbulent Kaimal wind fields and either regular or irregular waves. Good agreement is obtained at low TSR, region in which the Blade Element Momentum theory is known to be reliable. It has also been observed that discrepancies appear between the two theories at high TSR when the rotor is highly loaded with

strong interactions between the rotor and its wake, which cannot be accurately modelled by BEM codes.

REFERENCES

[1] P. J. Moriarty and A. C. Hansen, "AeroDyn Theory Manual," 2005.

[2] T. Sebastian and M. A. Lackner, "Characterization of the unsteady aerodynamics of offshore floating wind turbines," *Wind Energy,* 2013.

[3] J. M. Jonkman and W. Musial, "Offshore Code Comparison Collaboration (OC3) for IEA Task 23 Offshore Wind Technology and Deployment," *(Technical report) NREL/TP-5000-48191,* 2010.

[4] IEA Wind, "Task 30 : Offshore Code Comparison Collaboration Continuation (OC4)," [Online]. Available: https://www.ieawind.org/task_30/task30_Public.html. [Accessed 08 03 2017].

[5] IEA Wind, "IEA Wind 2014 Annual Report," 2015.

[6] A. Combourieu, M. Philippe, F. Rongère and A. Babarit, "InWave: a new flexible tool dedicated to Wave Energy Converters," *In Proceedings of the ASME 2014 33rd International Conference on Ocean, Offshore and Arctic Engineering, OMAE2014, June 8-13, 2014, San Francisco, California, USA,* 2014.

[7] National Renewable Energy Laboratory (NREL) (USA), "NWTC Information portal - FAST," [Online]. Available: https://nwtc.nrel.gov/FAST. [Accessed 2015 11 2015].

[8] I. Bayati, M. Belloli, L. Bernini and A. Zasso, "Wind tunnel validation of AeroDyn within LIFES50+ project: imposed Surge and Pitch tests," *In Proceedings of The Science of Making Torque from Wind (TORQUE 2016), Journal of Physics: Conference Series 753 (2016) 092001,* 2016.

[9] F. Blondel, R. Boisard, M. Milekovic, G. Ferrer, C. Lienard and D. Teixeira, "Validation and comparison of aerodynamic modelling approaches for wind turbines," *In Proceedings of the Science of Making Torque From Wind (TORQUE2016), Journal of Physics: Conference Series 753,* 2016.

[10] J. C. Murray and M. Barone, "The development of CACTUS, a wind and marine turbine performance simulation code," *in proceedings of 49th AIAA Aerospace Sciences Meeting,* 2011.

[11] A. Babarit and G. Delhommeau, "Theoretical and numerical aspects of the open source BEM solver NEMOH," *In Proceedings of the 11th European Wave and Tidal Energy Conference 6-11th Sept 2015, Nantes, France,* 2015.

[12] O. Faltinsen, "Sea Loads on Ships and Offshore Structures," *Cambridge University Press,* 1993.

[13] F. Rongère and A. H. Clément, "Systematic dynamic

modeling and simulation of multibody offshore structures: application to wave energy converters," *Proceedings of the ASME 2013 32nd International Conference on Ocean, Offshore and Artic Engineering, OMAE2013, June 9-14, 2013, Nantes, France, 2013.*

[14] NREL - NWTC Information Portal, "MAP++," NREL, [Online]. Available: https://nwtc.nrel.gov/MAP. [Accessed 29 06 2016].

[15] A. Combourieu, M. Philippe, A. Larivain and J. Espedal, "Experimental Validation of InWave, a Numerical Design Tool for WECs," *In Proceedings of the 11th European Wave and Tidal Energy Conference 6-11th Sept 2015, Nantes, France,* 2015.

[16] V. Leroy, A. Combourieu, M. Philippe, A. Babarit and F. Rongère, "Benchmarking of the new design tool InWave on a selection of wave energy converters from NumWEC project," *In Proceedings of the 2nd Asian Wave and Tidal Energy Conference 28-30th July 2014, Tokyo, Japan,* 2014.

[17] J. Jonkman, S. Butterfield, W. Musial and G. Scott, "Definition of a 5-MW Reference Wind Turbine for Offshore System Development," *Technical Report NREL/TP-500-39060, National Renewable Energy Laboratory,* 2009.

[18] J. M. Jonkman, A. Robertson and G. J. Hayman, "HydroDyn User's Guide and Theory Manual," *National Renewable Energy Laboratory (NREL),* 2016.

[19] A. K. Dev and J. A. Pinkster, "Viscous drift forces on semi-sumersibles," *The Royal Institution of Naval Architects, RINA, W193,* 2001.

[20] M. Jeon, S. Lee and S. Lee, "Unsteady aerodynamics of offshore floating wind turbines in platform pitching motion using vortex lattice method," *Renewable Energy,* 2014.

[21] NREL - NWTC Information Portal, "TurbSim," NREL, [Online]. Available: https://nwtc.nrel.gov/TurbSim. [Accessed 26 12 2016].